Thermal study on the synthesis of the doped ZnO to be used in TCO films

Suzana Mihaiu[1], Imre Miklós Szilágyi[2,3*], Irina Atkinson[1*], Oana Catalina Mocioiu[1], Dávid Hunyadi[3], Jeanina Pandele-Cusu[1], Alexandra Toader[1], Cornel Munteanu[1], Stefan Boyadjiev[2], János Madarász[3], György Pokol[3] and Maria Zaharescu[1]

[1]*Institute of Physical Chemistry "Ilie Murgulescu" of the Romanian Academy 202 Splaiul Independentei, 060021 Bucharest, Romania*

[2]*MTA-BME Technical Analytical Chemistry Research Group, H-1111 Budapest, Szt. Gellért tér 4, Hungary*

[3]*Department of Inorganic and Analytical Chemistry Budapest University of Technology and Economics, H-1521 Budapest, Szt. Gellért tér 4, Hungary*

Email: irinaatkinson@yahoo.com, Phone: +4021 318 85 95; fax +4021 312 11 47

imre.szilagyi@mail.bme.hu

Abstract

ZnO, Li doped and Li,Ni co-doped ZnO powders to be later used as transparent conductive oxide (TCO) thin film were prepared by heat treatment of gels obtained from alcoholic $Zn(CH_3COO)_2 \cdot 2H_2O$, $LiNO_3 \cdot nH_2O$ and $NiSO_4 \cdot 6H_2O$ solutions with $(CH_3CH_2OH)_3N$ as chelating agent. The properties of the powders and their thermal treatment were studied by thermogravimetric and termodifferential anlysis (TG/DTA), differential scanning calorimetry (DSC), evolved gas analysis coupled with mass spectroscopy (EGA-MS), Fourier transform infrared spectroscopy (FTIR), X-ray diffraction (XRD) and scanning electron microscopy coupled with energy dispersive X-ray (SEM/ EDX). The as-prepared gels consisted of submicron platelet-like particles and contained zinc acetate dihydrate and hydrozincite in different amount and with different preferred orientations. During annealing the gels, zinc-acetate decomposed between 110-350 °C with the release of CH_3COOH, acetone and CO_2. The N content of the chelating agent was responsible for NH_3 and NO evolution. The thermal behavior of the doped

gels was similar, but there were also differences in the mass losses, amount of released gases. Based on TG/DTA data, ZnO powders were obtained from the gels by annealing both at 275 and 500 °C. After heating at 275 °C, the obtained powders consisted of spherical 1-2 micron grains of wurtzite. The inclusion of the dopants was successful according to EDX and cell parameter data. Thermal study of the powder annealed at 275 °C confirmed that they still contain some zinc acetate. In the case of the doped samples the mass loss was smaller, since the Li and Ni dopants catalized the composition of zinc acetate during the previous annealing at 275 °C. After annealing the gels at 500 °C, stable un-doped ZnO or doped ZnO particles were obtained.

Keywords: ZnO, doping, gel, TCO, Li, Ni, p-type semiconductor

1. Introduction

Significant research efforts have been made in recent years in developing transparent doped and un-doped ZnO thin films, which are one of the strongest candidates in a variety of applications. Their main potential application is currently in transparent conductive oxide (TCO) coatings, window layers in solar cells, field emitters, ultraviolet laser emission, photodetectors, piezoelectricity, thermoelectric materials, bio-sensors, short wavelength light emitting diode and information technologies [1-3].

ZnO is a very promising material, due to its low toxicity, low cost and outstanding properties. It has wurtzite structure, it is an n-type direct wide band gap semiconductor (Eg =3.4 eV) with large excitation binding energy of 60 meV at room temperature, high Seebeck coefficient [4]. Both its optical and electronic characteristics can be controlled by the presence of dopants, which are selected depending on the required properties and applications. The typical dopants that have been used to improve the n-type ZnO performance are the group III elements of the periodic table (B, Al, In, Ga). However, for most optoelectronic devices, it is also necessary to have ZnO with p-type conductivity. Growth of p-type ZnO is highly challenging. In principle, p-type conductivity can be realized in ZnO by doping either with group IA and IB elements [Li, Na, K, Ag, Cu] to replace Zn or by doping with group V elements [N, P, As, Sb] in the place of oxygen [5-8].

Synthesis methods such as metal-organic chemical vapour deposition, atomic layer deposition, sol–gel method, spray pyrolysis, sputtering and pulsed laser deposition have been reported to prepare un-doped and doped ZnO films as n-type and p-type semiconductors for application as TCO [9]. Among them, the sol-gel method provides several advantages, i.e. easy control of the final materials, the possibility of deposition on complex-shaped substrates, easy control of dopant concentration and structural homogeneity, low temperature of thermal treatment of films, as well as the low cost of the used chemicals and equipments [10.11].

Our previous studies [12,13] reported Sn and Al doped ZnO thin films obtained by sol-gel method, which exhibited n-type semiconductor behavior, good optical transmittance and high conductivities. For most optoelectronic devices such as solid state light emitting diodes (LED) or lasers made of ZnO, it is necessary to have p-type ZnO. Obtaining p-type doping in ZnO has proved to be a very difficult task due to various reasons, such as deep acceptor level, low solubility of acceptor dopant and native donor defects like zinc interstitial (Zn_i) and oxygen vacancy (V_o). Recently, p-type Li doped ZnO and Li,Ni co-doped ZnO thin films on both glass and Si wafer substrates obtained by sol-gel route showing good transmittances (70-90%) from visible to near-IR range, and p-type semiconducting behaviour even after 4 months storage has been reported by our group [14]. The present work aims to investigate the thermal behaviour of the sol-gel precursors and formation of the intermediate compounds in order to establish a proper thermal treatment of p-type doped ZnO films. Understanding the decomposition of the precursors as well as the role of the dopants and native points defects (i.e. vacancies, interstitials, and antisites) is a key towards controlling the optical properties and conductivity of ZnO.

Hence, ZnO, Li doped and Li,Ni co-doped ZnO powders were prepared by heat treatment of gels obtained from alcoholic $Zn(CH_3COO)_2 \cdot 2H_2O$, $LiNO_3 \cdot nH_2O$ and $NiSO_4 \cdot 6H_2O$ solutions with $(CH_3CH_2OH)_3N$ as chelating agent. The properties of the powders and their thermal treatment were studied by TG/DTA, DSC, EGA-MS, FTIR, XRD and SEM-EDX methods.

2. Materials and methods

The starting materials (all reagent grade) for preparing alcoholic solutions were zinc acetate dihydrate - $Zn(CH_3COO)_2 \cdot 2H_2O$ (Merck), lithium nitrate - $LiNO_3 \cdot nH_2O$ (Merck), nickel

(II) sulfate hexahydrate - $NiSO_4 \cdot 6H_2O$ (Merck). Triethanolamine $(CH_3CH_2OH)_3N$ (BAKER ANALYZED) was used as chelating agent. Absolute ethanol (Merck) was used as solvent except to prepare the Ni solution, where methanol was used as solvent. The method of the alcoholic precursor solution preparation was presented previously [15]. The following precursor solutions have been obtained: 0.2 M of Zn^{2+} (S_Z); 0.2 M of 99 % at. Zn^{2+} and 1 % at. Li^+ (S_{ZL}); 0.2 M of 99 % at. Zn^{2+} with 0.05 % at. Li^+ and 0.05 % at. Ni^{2+} (S_{ZLN}). By solvent evaporation in air at room temperature un-doped ZnO (ZAD), Li doped ZnO (ZAD-Li) and Li, Ni co-doped ZnO (ZAD-Li,Ni) gels were obtained from the solutions S_Z, S_{ZL} and S_{ZLN}, respectively. Based on TG/DTA results, the as-prepared gels were thermally treated under isothermal conditions for one hour at 275 °C and 500 °C.

The thermal evolution of the gels and powders were studied by TG/DTA and DSC with a Mettler Toledo TGA/SDTA 851^e equipment and a Mettler Toledo 823^e DSC instrument using 5 °C min^{-1} heating rate. The evolved gas analytical measurements were studied by an STD 2960 Simultaneous DTA/TGA (TA Instruments Inc.) thermal analyzer using a heating rate of 5 °C min^{-1} and Pt crucibles. The furnace was purged with air atmosphere (130 ml min^{-1}). Evolved gas analytical (EGA) curves were recorded by a Thermostar GSD 200 (Balzers Instruments) quadrupole mass spectrometer (MS). A mass range between m/z = 1-64 was monitored through 64 channels in Multiple Ion Detection Mode (MID) with a measuring time of 0.5 s $channel^{-1}$. Further details of the TG/DTA-MS setup are described in other studies [15,16].

FT-IR spectra for gels and powders were recorded with a Nicolet 6700 apparatus in 400-4000 cm^{-1} domain. The spectra were recorded in transmittance mode and the powders were imobilised in KBr pellets. The sensitivity of measurements was of 4 cm^{-1}.

X-ray diffraction measurements were performed using a Rigaku Ultima IV difractometer in parallel beam geometry equipped with CuKα radiation (wavelength 1.5406 Å). The XRD patterns were collected in 2Θ range between 10 to 70 with a speed of 5º min^{-1} and a step size of 0.02º. PDXL software from Rigaku, connected to ICDD database was used for phase identification and lattice parameters calculation. The lattice parameters were refined by whole-powder pattern fitting method (WPPF) using the split pseudo-Voigt profile function and B-spline background model. The crystallite size was determined using Williamson-Hall method.

Sample morphology was characterized by scanning electron microscopy (SEM) using a high-resolution microscope, FEI Quanta3 DFEG model, at an accelerating voltage of 5kV, in high vacuum mode with Everhart–Thornley secondary electron (SE) detector coupled with energy dispersive X-ray (EDX) analysis (standardless). Samples preparation was minimal and consisted in immobilizing the material on a double-sided carbon tape, without coating.

3. Results and disscusion

3.1. Reagents used

The reagents used for the sample preparation were characterized by TG/DTA from the point of view of their thermal stability. The mass losses and the corresponding thermal effects are summarized in Table 1. One may notice a rather good agreement between the calculated and experimental results obtained.

Table 1

In Figure 1 the XRD patterns of the starting reagents are shown. The diffraction lines were indexed according to JCPDS files: 00-033-1464 ($Zn(CH_3COO)_2 \cdot 2H_2O$), 00-047-1811($NiSO_4 \cdot 6H_2O$), 01-080-0203 ($LiNO_3$) and 00-024-0645 ($LiNO_3 \cdot 3H_2O$).

Fig. 1.

In Figure 2 the FTIR spectra for the reagents used for the sample preparation are presented. The spectrum of the hydrate nickel sulfate shows two bands at 3440 cm^{-1} and 1640 cm^{-1} for water; the bands at 1100 cm^{-1} and 672 cm^{-1} for SO_4^{2-} groups and the bands at 788 cm^{-1} and 475 cm^{-1} assigned to vibrations of Ni-O bonds. The spectrum of the hydrate lithium nitrate presents a broad band between 3600 and 3100 cm^{-1} and a peak at 1636 cm^{-1} assigned to water, while the bands at 1350 cm^{-1} and below 815 cm^{-1} to NO_3^- groups. In the spectrum of the hydrated zinc acetate the following bands are identified: the bands between 3600 and 3200 cm^{-1} associated with the stretching mode of water; the characteristic bands of asymmetric and symmetric stretchings of C=O bond in the acetate group at 1558 cm^{-1} and 1447 cm^{-1}; two bands at 1020 cm^{-1} and 954 cm^{-1} assigned to asymmetric and symmetric stretchings of C-O bond in the acetate group and the characteristic bands of the Zn-O vibrations at 695 and 622 cm^{-1}.

Fig. 2.

3.2. As-prepared gel and powder samples

Using the reagents and the experimental conditions presented above, gels were obtained successfully in the case of all three compositions studied.

Fig. 3.

Figure 3 shows the morphology of the ZAD-Li,Ni as-prepared gel. The largest portion of the gel is agglomerated, but some platelet-like particles were also noticed.

Figure 4 shows the XRD patterns of the as-prepared samples. In the as prepared samples the phases revealed by XRD were mainly composed of hydrozincite (JCPDS 00-072-1100) and zinc acetate dihydrate (JCPDS 00-033-1464). The doping changed significantly the ratio of these phases in the gels. The main constituent of the ZnO gel was zinc acetate dihydrate with small amount of hydrozincite, while the ratio of the two phases was just the opposite in the case of the ZAD-Li and ZAD-Li,Ni gels. In additon, there was difference in the preferred orientation of the Li and Li,Ni co-doped samples.

Fig. 4.

In Figure 5 the FT-IR spectra of as-obtained ZAD, ZAD-Li and ZAD-Li,Ni gel samples are presented. The bands identified in the FT-IR spectra of as-prepared samples in the 3600-2500 cm^{-1} region correspond to vibration of N-H, O-H and C-H bonds [17-20], which showed considerable differences between the samples. In the 1300-1581 cm^{-1} region two bands are assigned to symmetric and asymmetric stretching of C=O bond in the acetate group. In the 1010-1145 cm^{-1} region the observed bands are explained as the symmetric and asymmetric stretching modes of C-O bond in the acetate group. Below 686 cm^{-1} the bands are due to Zn-O vibration [17-22]. In the spectra of the doped samples the intensity of the Zn-OH band at 623cm^{-1} increased, and the bands at 502 and 420 cm^{-1} became more intense.

Fig. 5.

The thermal decomposition of zinc acetate dihydrate was investigated in detail previously [23-28]. It was found that the zinc acetate dihydrate decomposed in two steps, below 100 °C the

adsorbed water evolved, then between 150-300 °C the anhydrous zinc acetate decomposed, resulting in ZnO. During the decomposition CH_3COOH, acetone and CO_2 evolution was reported [26-28].

The zinc acetate dihydrate component of the samples decomposed, as it was expected (Fig. 6). The first step occured below 100 °C, as water evolved in an endothermic process causing a 2.28 % mass change. In the second step (110-350 °C) the anhydrous zinc acetate decomposed in an endothermic reaction (295 °C), above 300 °C there were exothermic peaks (302, 316 °C) due to the combustion of the organic components. From the zinc acetate, first CH_3COOH evolved, then above 260 °C acetone and CO_2 were released from the decomposition of the acetate ion [26-28]. The H_2O evolution during this step could be explained by the burning of the organic contents of the zinc acetate and other components. The N content of the sample decomposed as-well in this step, resulting in NH_3 and NO evolution. In the third step (370-490 °C) the mass loss was 11,8 % accompanied by an exothermic reaction, and probably the other residual organic components decomposed and combusted, since during this step only H_2O, CO_2 and NO evolved.

Fig. 6.

The thermal decompositions of the as-obtained ZAD, ZAD-Li and ZAD-Li,Ni gel samples show similar behaviour, but some differences were noticed (Fig. 7).

The TG and MS curves showed, that the ZAD-Li,Ni sample contained the largest amount of water (10.71 %), and the ZAD-Li sample also contained more water (5.42 %), than the ZAD sample (2.38 %). The rate of decomposition was also somewhat different during the second decomposition step. The presence of doping agents may catalyzed the decomposition, since between 150-250 °C the doped samples (ZAD-Li, ZAD-Li,Ni) exhibited larger mass loss, than the un-doped sample (ZAD). In the case of the ZAD-Li,Ni sample the main mass loss occurred around 280 °C, with 20 °C lower, than in the case of the other two samples. For ZAD-Li and ZAD-Li,Ni samples NH_3 and acetone evolved besides the gases, which were observed during the decomposition of the ZAD sample at this temperature range. Some of the evolved NH_3 has combusted into NO. Also, during this decomposition step the amount of the evolved CH_3COOH was greater in the case of the ZAD-Li and ZAD-Li,Ni samples. During the third step (370-490

°C), from the ZAD-Li sample a small amount of NH_3 evolved, and most of the evolved NH_3 combusted into NO, while from the other two samples only a small amount of NO evolved. At the end of the measurement the mass of the doped samples was greater (ZAD-Li: 32.84 %, ZAD-Li,Ni: 33.10 %), than the un-doped sample (28.60 %).

Fig. 7.

3.3. Samples annealed at 275 °C

Based on the TG/DTA curves of the as-prepared samples, they were thermally treated at two different tempartures in order to establish the mechanism of their thermal decomposition. After thermal treatment at 275 ^{o}C all obtained powders presented gray color and spherical grains.

In Figure 8 the SEM image and EDX spectrum (inset of Fig.8) of the ZAD-Li, Ni precursor powder thermally treated at 275 °C for 1 h is presented. According to SEM, spherical grains were obtained. EDX analysis revealed the presence of Ni used as co dopant. Li could not be observed, because EDX is not capable to detect it.

Fig. 8.

Figure 9 shows the XRD pattern of the ZAD-Li,Ni powder thermally treated at 275 °C. At this temperature a partially crystallised sample was obtained, in which ZnO crystals with wurtzite (hexagonal) structure (according to JCPDS card 00-036-1451) formed, accompanied with a smaller portion of an amorphous phase. The amorphous phase was confirmed by the characteristic broad halo at around $2\theta \approx 25°$ in the diffraction pattern. No preferential orientations and secondary diffraction peaks were observed.

Fig. 9.

In the FT-IR spectrum of the ZAD precursor, thermally treated at 275 °C the broad absorption band between 3060-3600 cm^{-1} is due to the presence of O-H stretching mode of the hydroxyl group as shown in Figure 10. The bands appearing at 2928 and 2872 cm^{-1} are characteristic to CH_2 stretching mode. The acetate bands appear at 1589 cm^{-1} and 1400 cm^{-1} for C=O bonds and at 1114 cm^{-1} and 1022 cm^{-1} for C-O bonds. The translation vibrations of Zn-OH are observed at 674 and 621 cm^{-1} [18-20]. The absorption band around 444 cm^{-1} is due to Zn-O

vibration mode [20-22]. The FT-IR spectra of ZAD-Li and ZAD-Li,Ni samples, thermally treated at 257 ^{o}C, show similar behavior with undoped sample, as can be seen in the Figure 10.

Fig. 10.

The thermal decomposition of the un-doped ZnO precursor thermally treated at 275 °C (Fig. 11) showed that small amount of adsorbed water was released until 150 °C. The sample still contained some zinc acetate; thus, between 110-350 °C CH_3COOH evolved, and some of the evolved CH_3COOH decomposed into acetone and CO_2. At this temperature range NH_3 evolved as-well from the organic matrix of the sample. Some of the evolved gases combusted, resulting in H_2O, CO_2 and NO. Between 440-500 °C the organic matrix decomposed (NH_3) and combusted (H_2O, CO_2, NO). At this temperature range no CH_3COOH nor acetone evolution could be detected. The thermal decomposition of this sample was very similar to the untreated sample, the only difference was the greater mass % values after each step, since some of the zinc acetate already decomposed into ZnO due to the thermal treatment.

Fig. 11.

The thermal decompositions of the treated samples were very similar (Fig. 12). One of the differences was that the final mass of the doped samples was greater (ZAD-Li: 61.33 %, ZAD-Li,Ni: 64.82 %), than the mass of the un-doped sample (52.17 %). This behaviour could be explained by the fact that during the thermal treatment at 275 °C the doped samples decomposed in larger quantities into ZnO, since the Li and Ni doping may have catalyzed this reaction. The doping agents could also catalyzed the decomposition of CH_3COOH, since in case of the ZAD-Li and ZAD-Li,Ni samples only traces of CH_3COOH could be detected, most of the CH_3COOH being decomposed into acetone.

Fig. 12.

This study brings important information on the structure and morphology of the samples thermally treated at 275 °C. This is very important to obtain films with p-type semiconductivity on the substrate that can not be thermally treated over 300 °C, as for example the Au substrate.

3.4. Samples annealed at 500 °C

By thermal treartment at 500 ^{o}C white powders were obtained. The SEM image of the ZAD-Li, Ni powder is shown in Figure 13. The size of the particles decreased, compared to the powders obtained at 275 ^{o}C, and the grains were composed of smaller particles. EDX (inset of Fig. 13) clearly confirmed the presence of the dopant Ni, while Li was again theoretically not able to be detected by EDX. In our previous study [14] the presence of Ni in the composition of the Li,Ni co-doped ZnO thin film thermally treated at 500 °C, has been confirmed by XPS characterization and by XRF measurement on the Li,Ni co-doped ZnO powder, thermally treated at the same temeparture.

Fig. 13.

Figure 14 shows the XRD pattern of the ZAD-Li,Ni thermally treated at 500^{o}C. The lattice parameters and the crystallite size of the ZAD-Li,Ni powders thermally treated at different temperature are listed in Table 2. It can be observed that lattice parameters are slightly smaller than those of pure ZnO. The change of lattice parameters could be attributed to the small incoproration of Li and Ni into ZnO network due to the difference between the ionic radius of the elements (rZn^{2+} = 0.74Å, rLi^{+}=0.60 Å and rNi^{2+} = 0.69Å) [29,30].

Fig. 14.

Table 2

In Figure 15 the FT-IR spectra of the samples thermally treated at 500ºC are presented. The bands in the low frequency region 429–485 cm^{-1} correspond to the lattice vibration mode of Zn-O [18-22] for doped and un-doped samples. The bands are shifted to lower wavenumbers in doped samples. Small bands at 1507 cm^{-1} and 1123 cm^{-1} are assigned of organic adsorbed species [18-22].

Fig. 15.

The DTA/TGA curves as well as the corresponding EGA results for the ZAD-500, ZAD-Li-500 and ZAD-Li,Ni-500 did not show any change upon annealing. This result underlyins the thermal stablity of the resulted powders.

Based on the comparative results obtained at 275 °C and 500 °C, the complet thermal decomposition of the samples occured only after 500 °C. The behaviour is similar for the un-

doped and Li and Li, Ni co-doped ZnO, underlying that the dopands do not change esentially the thermal behaviour of the studied samples.

Conclusions

In this study, un doped ZnO (ZAD), Li doped (ZAD-Li) and Li,Ni co-doped ZnO (ZAD-Li,Ni) powders were prepared by heat treatment of gels obtained from alcoholic $Zn(CH_3COO)_2 \cdot 2H_2O$, $LiNO_3 \cdot nH_2O$ and $NiSO_4 \cdot 6H_2O$ solutions with $(CH_3CH_2OH)_3N$ as chelating agents. The properties of the powders and their thermal treatment were studied by TG/DTA, DSC, EGA-MS, FTIR, XRD and SEM-EDX.

The as-prepared gels consisted of submicron platelet-like particles and contained zinc acetate dihydrate and hydrozincite in different amount and with different preferred orientations. During annealing the gels, zinc-acetate decomposed between 110-350 °C with the release of CH_3COOH, acetone and CO_2. The N content of the chelating agent was responsible for NH_3 and NO evolution. The thermal behavior of the doped gels was similar, but there were also differences in the mass losses and amount of released gases.

Based on TG/DTA data, ZnO powders were obtained from the gels by annealing both at 275 and 500 °C, but at 275 °C the samples still contained some zinc acetate residues. After heating at 275 °C, the obtained powders consisted of spherical 1-2 micron grains of wurtzite. In the case of the doped samples the mass loss was smaller, since the Li and Ni dopants catalyzed the decomposition of zinc acetate during the previous annealing at 275 °C. After annealing the gels at 500 °C, stable un-doped or doped ZnO particles were obtained. The inclusion of the dopants was successful according to XRD and EDX results.

Our results suggest that p-tye Li and Li,Ni co-doped ZnO can be prepared by annealing precursors gels already at 275 °C. This is convenient if heat sensitive substrates are covered by doped zinc based gels using dip coating, spin coating, etc; however, in this case the as-obtained doped ZnO TCO films will still contain some residual precursors. To completely remove them an annealing at 500 °C is needed.

Acknowledgments

The financial support of EU (ERDF) INFRANANOCHEM-No. 19/01.03.2009 project is gratefully acknowledged.

I. M. S. thanks for a János Bolyai Research Fellowship of the Hungarian Academy of Sciences and an OTKA-PD-109129 grant. S. B. acknowledges the Postdoctoral Fellowship programme of the Hungarian Academy of Sciences (2013-2015).

References

[1] Lee JY, Lee JH, Kim HS, Lee CH, Ahn HS, Cho HK, Kim YY, Kong B, Lee HS. A study on the origin of emission of the annealed n-ZnO/p-GaNheterostructure LED. Thin Solid Films. 2009;517:5157-60.

[2] Hassan JJ, Mahdi MA, Yusof Y, Abu-Hassan H, Hassan Z, Al-Attar HA, Monkman AP. Fabrication of ZnO nanorod/p-GaN high-brightness UV LED by microwave-assisted chemical bath deposition with $Zn(OH)_2$–PVA nanocomposites as seed layer. Opt Mater. 2013;35:1035-41.

[3] Malek MF, Mamat MH, Khusaimi Z, Sahdan MZ, Musa MZ, Zainun AR, Suriani AB, Md Sin ND, Abd Hamid SB, Rusop M. Sonicated sol–gel preparation of nanoparticulate ZnO thin films with various deposition speeds: The highly preferred c-axis (0 0 2) orientation enhances the final properties. J Alloy Compd. 2014;582:12–21.

[4] Qu X, Wang W, Shuchen Lv, Jia D. Thermoelectric properties and electronic structure of Al-doped ZnO. Solid State Comm. 2011;151:332-6.

[5] Janotti A, Van de Walle CG. Fundamentals of zinc oxide as a semiconductor. Rep Prog Phys. 2009;72:126501.

[6] Li L, Shan CX, Li BH, Yao B, Zhang JY, Zhao DX, Zhang ZZ, Shen DZ, Fan XW, Lu YM. The compensation source in nitrogen doped ZnO. J Phys D: Appl Phys. 2008;41:245402.

[7] Yao B, Xie YP, Cong CX, Zhao HJ, Sui YR, Yang T, He Q. Mechanism of p-type conductivity for phosphorus-doped ZnO thin film. J Phys D: Appl Phys. 2009; 42:015407.

[8] Yu D, Hu L, Qiao S, Zhang H, Len SEA, Len LK, Fu Q, Chen X, Sun K. Photoluminescence study of novel phosphorus-doped ZnO nanotetrapods synthesized by chemical vapor deposition. J Phys D:Appl Phys. 2009;42:055110.

[9] Díez-Betriu X, Jiménez-Rioboo R, Sánchez- Marcos J, Céspedes E, Espinosa A, de Andrés A. Amorphous-nanocrystalline Al doped ZnO transparent conducting thin films. J Alloy Compd. 2012;536S1:S445-9.

[10] Zi-qiang X, Hong D, Yan L, Hang C. Al-doping effects on structure, electrical and optical properties of c-axis-orientated ZnO:Al thin films. Mater Sci in *Semiconductor Processing* 2006;9:132-5.

[11] Casanova JR, Heredia EA, Bojorge CD, Canepa HR, Kellermann G, Craievich AF. Structural characterization of supported nanocrystalline ZnO thin films prepared by dip-coating. Appl Surf Sci 2011;257:10045–51.

[12] Toader Al., Mihaiu S., Voicescu M., Anastasescu M., Stroescu H., Nicolescu M., Atkinson I., Gartner M., Zaharescu M. Optical investigations of tin and zinc oxides as TCOs films. Proc. of SPIE. 2012; 8411-84111U:1-6.

[13] Mihaiu S., Toader A., Anastasescu M., Gabor M., Petrisor T. Jr., Stoica M., Zaharescu M. Al-doped and undoped zinc oxide fi lms obtained by soft chemistry. Processing and Application of Ceramics. 2009; 3(1-2): 79-84.

[14] Zaharescu M., Mihaiu S., Toader A., Atkinson I., Moreno J. C., Anastasescu M., Nicolescu M., Duta M., Gartner M., Vojisavljevic K., Malic B., Ivanov V. A., Zaretskaya, E. P. ZnO based transparent conductive oxide films with controlled type of conduction. Thin Solid Films. 2014; 571: 724-31.

[15] Prasad R. L., Kushwaha A., Szilágyi I. M., Kótai L. Solid state thermal degradation behaviour of 1-D coordination polymers of Ni(II) and Cu(II) bridged by conjugated ligand. J Therm Anal Calorim. 2013; 114: 653-64.

[16] Szilágyi I. M., Deák A., Várhelyi jr. C., Madarász J., Pokol G., Gömöry Á., Várhelyi C. Structural and thermal study of assymetric α-dioxime complexes of Co(III) with Cl and methyl-pyridines. Polyhedron. 2010; 10: 2185-9.

[17] Mihaiu S, Atkinson I, Anastasescu M, Toader A, Voicescu M, Zaharescu M. Spectroscopic investigations of the formation of the Zn-Sn-O nanostructured films. Rev Roum Chim. 2012;57:477-90.

[18] Zaharescu M, Mocioiu OC. Chapter 9 Infrared spectroscopy. In book:Chemical solution deposition of functional oxide thin films. Editors: Schneller T, Waser R, Kosec M, Payne D. Springer-Verlag Wien; 2013, p. 213-230.

[19] Mihaiu S, Gartner M, Voicescu M, Mocioiu OC**,** Zaharescu M. Characterization of the ZnO thin films obtained by chemical route. Opt Adv Mater-RC. 2009;3:884-90.

[20] Mihaiu SM, Madarasz J, Pokol G, Szilagyi IM, Kaszas T, Mocioiu OC**,** Atkinson I, Toader A, Munteanu C, Marinescu VE, Zaharescu M. Thermal behavior of ZnO precursor powders obtained from aqueous solutions. Rev Roum Chim. 2013;58:335-45.

[21] Subhan MA, Ahmed T, Uddin N, Azad AK, Begum K. Synthesis, characterization, PL properties, photocatalytic and antibacterial activities of nano multi-metal oxide NiO-CeO_2-ZnO, Spectrochim Acta Part A: Molecular and Biomolecular Spectroscopy 2015;136:824-31.

[22] Awad MA, Ibrahim EMM, Ahmed AM, Synthesis and thermal stability of ZnO nanowires, J Therm Anal Calorim. 2014; 117: 635-42

[23] Farbod M, Jafarpoor E, Hydrothermal synthesis of different colors and morphologies of ZnO nanostructures and comparison of their photocatalytic properties, Ceram. Int. 2014; 40: 6605-10.

[24] Ghule AV, Lo B, Tzing SH, Ghule K, Chang H, Ling YC, Simultaneous thermogravimetric analysis and in situ thermo-Raman spectroscopic investigation of thermal decomposition of zinc acetate dihydrate forming zinc oxide nanoparticles, Chem. Phys. Lett. 2003;381:262-70.

[25] Saravanan R, Thirumal E, Gupta VK, Narayanan V, Stephen A, The photocatalytic activity of ZnO prepared by simple thermal decomposition method at various temperatures, J Mol Liq. 2013;177:394-401.

[26] Duan Y, Li J, Yang X, Hua L, Wanga Z, Liu Y, Cunxin Wang, Kinetic analysis on the non-isothermal dehydration by integral master-plots method and TG–FTIR study of zinc acetate dihydrate, J. Anal. Appl. Pyrolysis. 2008;83:1-6.

[27] Lin CC, Li YY, Synthesis of ZnO nanowires by thermal decomposition of zinc acetate dihydrate. Mater. Chem. Phys.. 2009;113:334-337.

[28] Mereu RA, Mesaros A, Petrisor Jr. T, Gabor M, Popa M, Ciontea L, Petrisor T, Synthesis, characterization and thermal decomposition study of zincpropionate as a precursor for ZnO nano-powders and thin films, J. Anal. Appl. Pyrolysis. 2013;104:653-659.

[29] Caglar M, Caglar Y, Aksoy S, Ilican S. Temperature dependence of the optical band gap and electrical conductivity of sol–gel derived undoped and Li-doped ZnO films. Appl Surf Sci 2010;256:4966-71.
[30] Yan X, Hu D, Li H, Li L, Chong X, Wang Y. Nanostructure and optical properties of M doped ZnO (M=Ni, Mn) thin films prepared by sol–gel process. Phys B. 2011; 406:3956-62.

Table 1. Thermal behavior of the starting reagents

Reagents		Thermal effects/ °C		Temperature range/ °C	Mass loss/ %		
		Exo	Endo		Exp.	Calculated	Products
1	$Zn(CH_3COO)_2 \cdot 2H_2O$	338 351	97 254	20-400	62.37	62.9	ZnO
2	$LiNO_3 \cdot nH_2O$	629	252 603	20-630	80.19	78.33	Li_2O
3	$NiSO_4 \cdot 6H_2O$	105 151 765		20-800	72.19	71.58	NiO

Table 2. Lattice parameters and crystallite size of the Li, Ni co-doped ZnO powders

Sample	*Lattice parameters/ Å*			*c/a*	*Crystallite size/ Å*	*S*	*Rwp*
	a	*b*	*c*				
ZAD-Li-Ni- 275 °C	3.2478	3.2478	5.2098	1.6041	178	1.041	5.72
ZAD-Li-Ni- 500 °C	3.2490	3.2490	5.2062	1.6024	185	1.063	7.43
ZnO -JCPDS 00-036-1451	3.2498	3.2498	5.2066	1.6021	-	-	

Where: S-the goodness of fit (between 1-1.5); Rwp- weighted difference between measured and calculated values (ideally should be around 10)

Caption of figures

Fig. 1. XRD patterns of the starting reagents

Fig. 2. FTIR spectra of the starting reagents

Fig. 3. SEM image of the ZAD-Li,Ni as-prepared sample

Fig. 4. XRD patterns of the as-prepared samples

Fig. 5. FT-IR spectra of as-prepared samples

Fig. 6. TG/DTA and evolved gas analytical MS ion current curves in air of the ZAD sample

Fig. 7. Comparison of the TG and evolved gas analytical MS ion current curves of the ZAD, ZAD-Li and ZAD-Li,Ni samples

Fig. 8. SEM image and EDX analysis (inset graph) of the ZAD-Li,Ni sample thermally treated at 275 °C

Fig. 9. XRD pattern of the ZAD-Li,Ni sample thermally treated at 275 °C

Fig. 10. FT-IR spectra of powders thermally treated at 275 ºC

Fig. 11. TG/DTA and evolved gas analytical MS ion current curves in air of the ZAD sample thermally treated at 275 °C

Fig. 12. Comparison of the TG and evolved gas analytical MS ion current curves of the ZAD, ZAD-Li and ZAD-Li,Ni samples thermally treated at 275 °C

Fig. 13. SEM image and EDX analysis (inset graph) of the ZAD-Li,Ni sample thermally treated at 500°C for 1 h.

Fig. 14. XRD pattern of the ZAD-Li,Ni sample thermally treated at 500 °C

Fig. 15. FT-IR spectra of powders thermally treated at 500 ºC

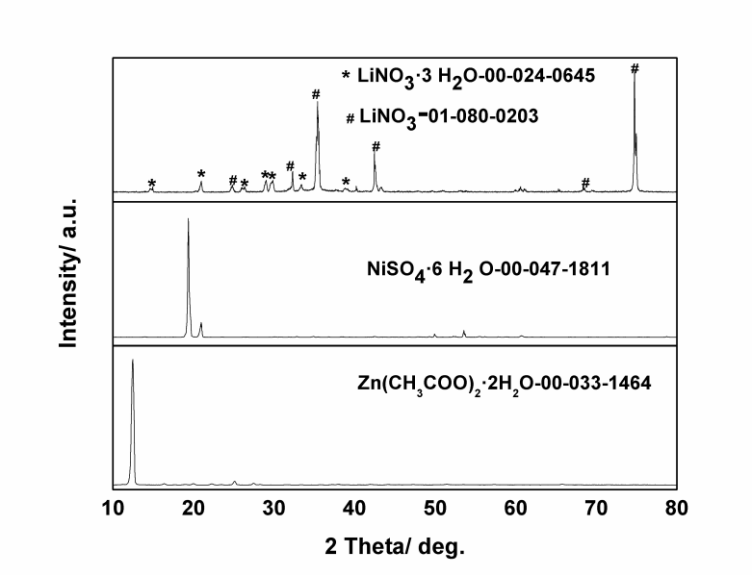
* LiNO3·3 H2O-00-024-0645
# LiNO3-01-080-0203
NiSO4·6 H2 O-00-047-1811
Zn(CH3COO)2·2H2O-00-033-1464
Intensity/ a.u.
10
20
30
40
50
60
70
80
2 Theta/ deg.

Fig. 1

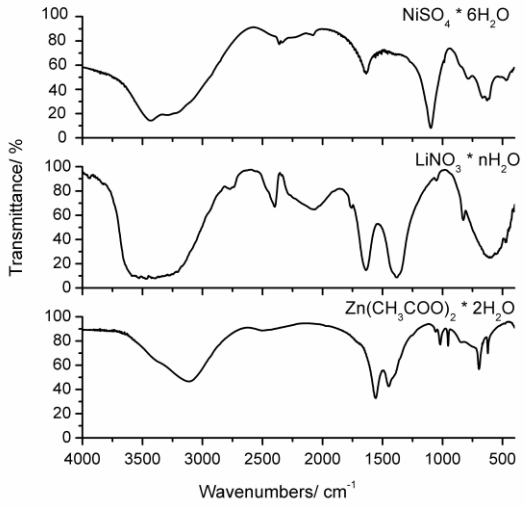
NiSO4 * 6H2O
LiNO3 * nH2O
Zn(CH3COO)2 * 2H2O
Transmittance/ %
100
80
60
40
20
0
4000
3500
3000
2500
2000
1500
1000
500
Wavenumbers/ cm-1

Fig. 2

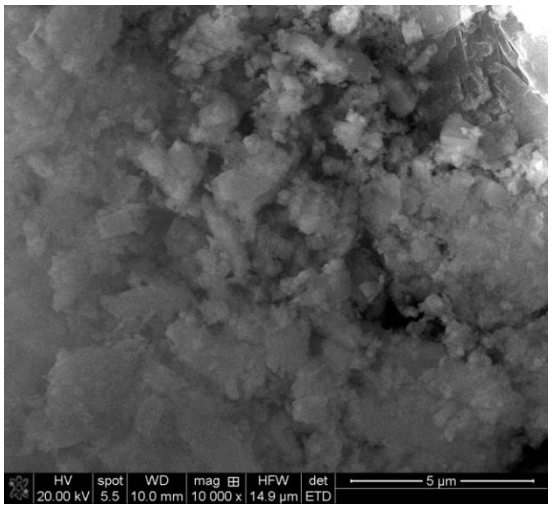
HV
20.00 kV
spot
5.5
WD
10.0 mm
mag
10 000 x
HFW
14.9 µm
det
ETD
5 µm

Fig. 3

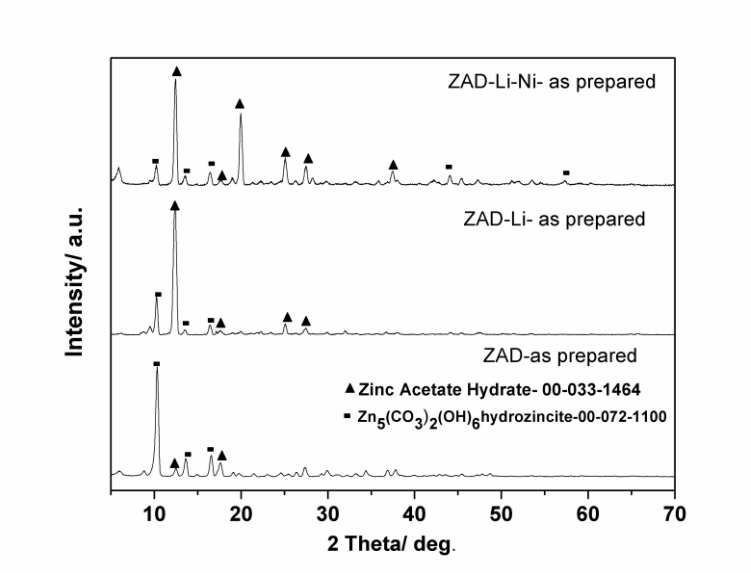
ZAD-Li-Ni- as prepared
ZAD-Li- as prepared
ZAD-as prepared
▲Zinc Acetate Hydrate- 00-033-1464
▪ Zn5(CO3)2(OH)6hydrozincite-00-072-1100
Intensity/ a.u.
10
20
30
40
50
60
70
2 Theta/ deg.

Fig. 4

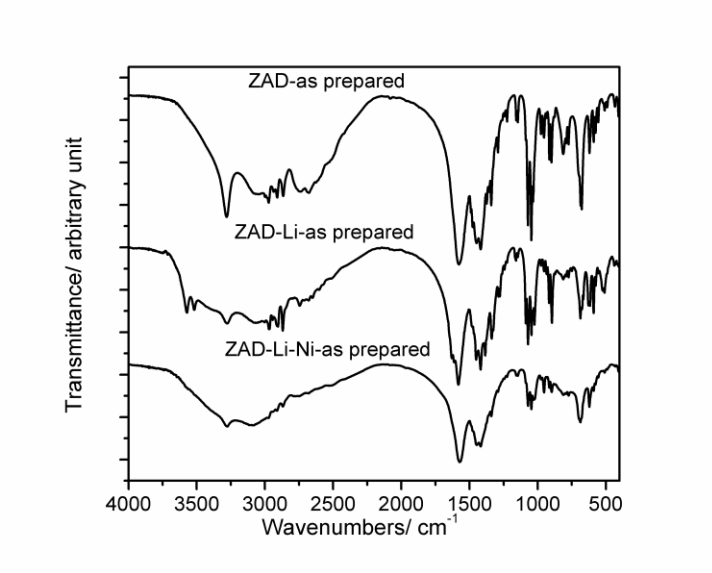
ZAD-as prepared
ZAD-Li-as prepared
ZAD-Li-Ni-as prepared
Transmittance/ arbitrary unit
4000
3500
3000
2500
2000
1500
1000
500
Wavenumbers/ cm-1

Fig. 5

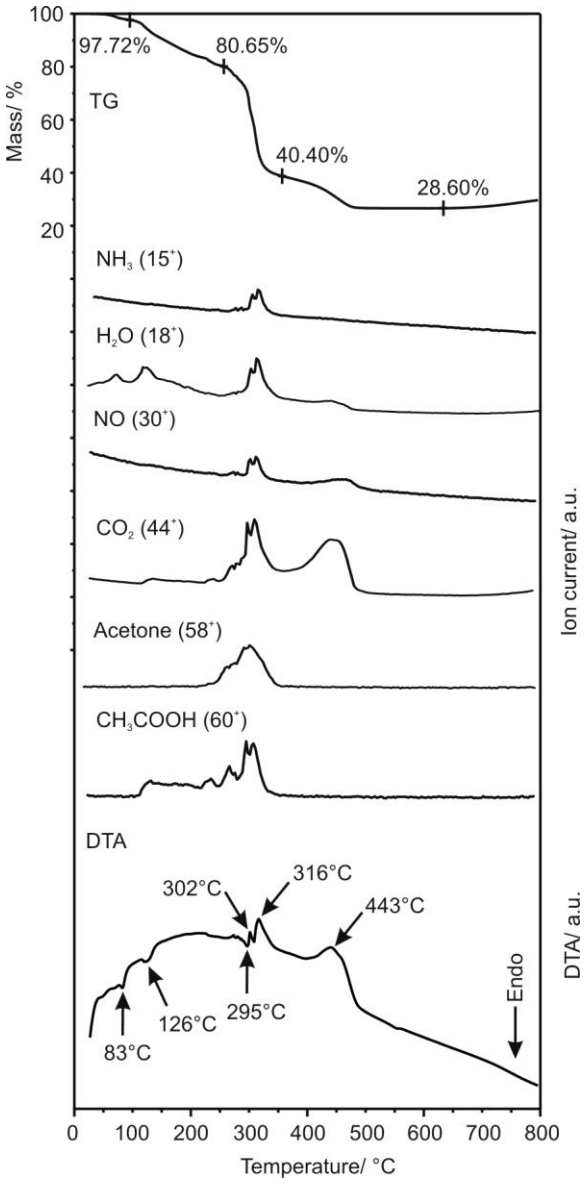
100
80
60
40
20
Mass/ %
97.72%
80.65%
40.40%
28.60%
TG
NH3 (15+)
H2O (18+)
NO (30+)
CO2 (44+)
Acetone (58+)
CH3COOH (60+)
Ion current/ a.u.
DTA
302°C
316°C
443°C
126°C
295°C
83°C
Endo
DTA/ a.u.
0
100
200
300
400
500
600
700
800
Temperature/ °C

Fig. 6

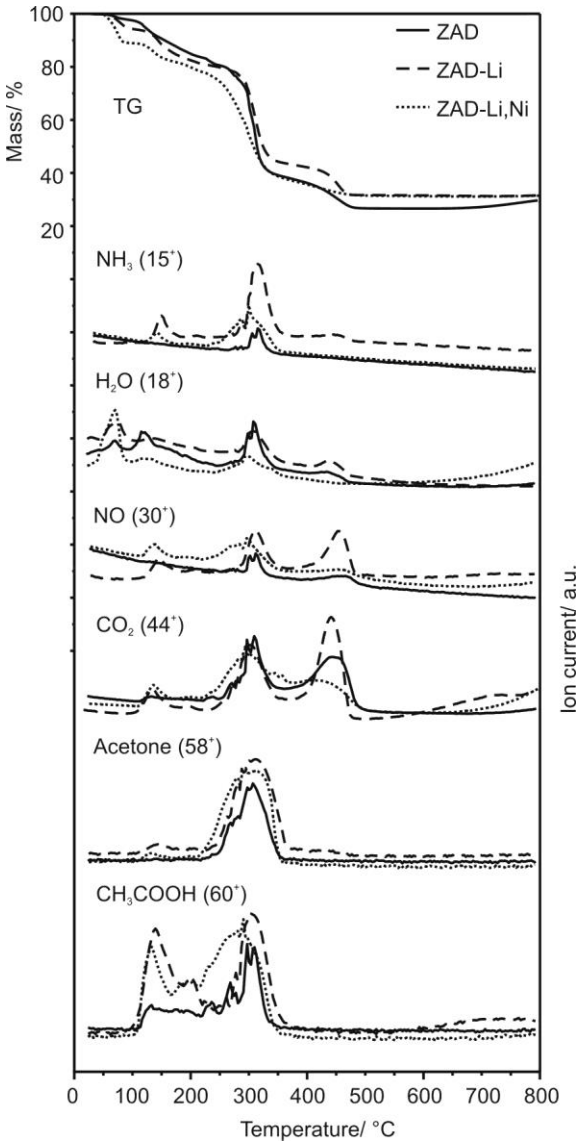
ZAD
ZAD-Li
ZAD-Li,Ni
TG
Mass/ %
100
80
60
40
20
NH3 (15+)
H2O (18+)
NO (30+)
CO2 (44+)
Acetone (58+)
CH3COOH (60+)
Ion current/ a.u.
0
100
200
300
400
500
600
700
800
Temperature/ °C

Fig. 7

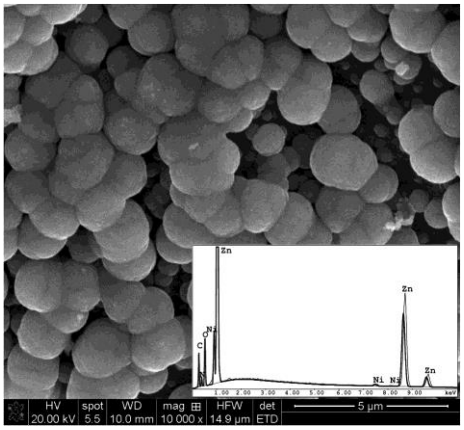
Zn
C
Ni
Zn
Ni Ni
Zn
HV
20.00 kV
spot
5.5
WD
10.0 mm
mag
10 000 x
HFW
14.9 µm
det
ETD
5 µm

Fig. 8

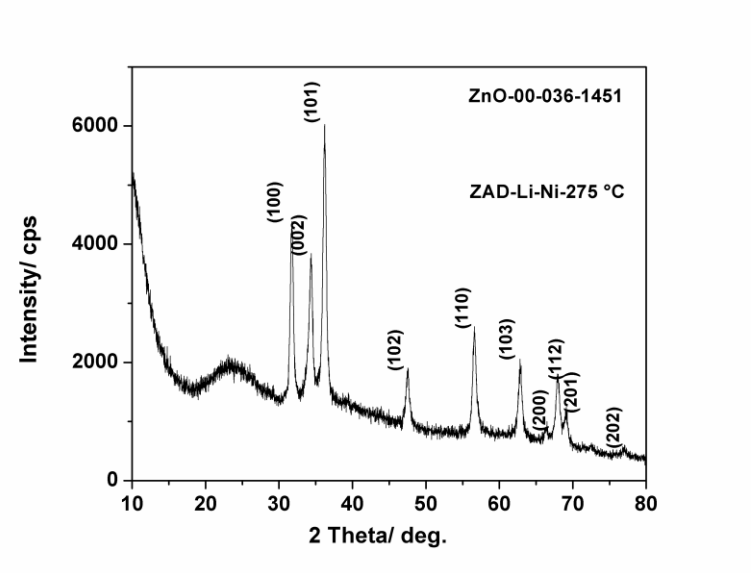
ZnO-00-036-1451
ZAD-Li-Ni-275 °C
Intensity/ cps
2 Theta/ deg.
(100)
(002)
(101)
(102)
(110)
(103)
(200)
(112)
(201)
(202)
0
2000
4000
6000
10
20
30
40
50
60
70
80

Fig. 9

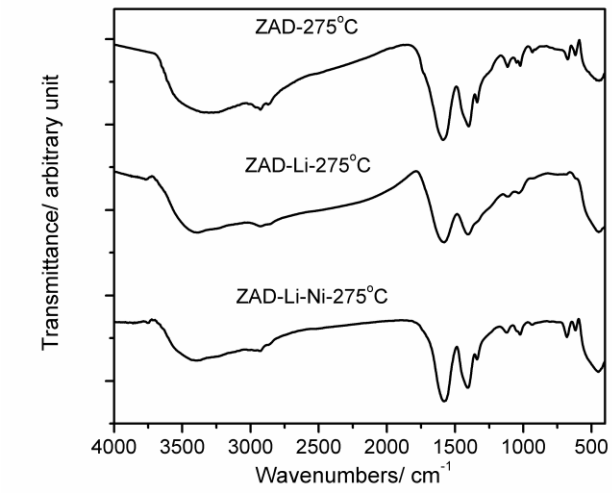
ZAD-275°C
ZAD-Li-275°C
ZAD-Li-Ni-275°C
Transmittance/ arbitrary unit
Wavenumbers/ cm-1
4000
3500
3000
2500
2000
1500
1000
500

Fig. 10

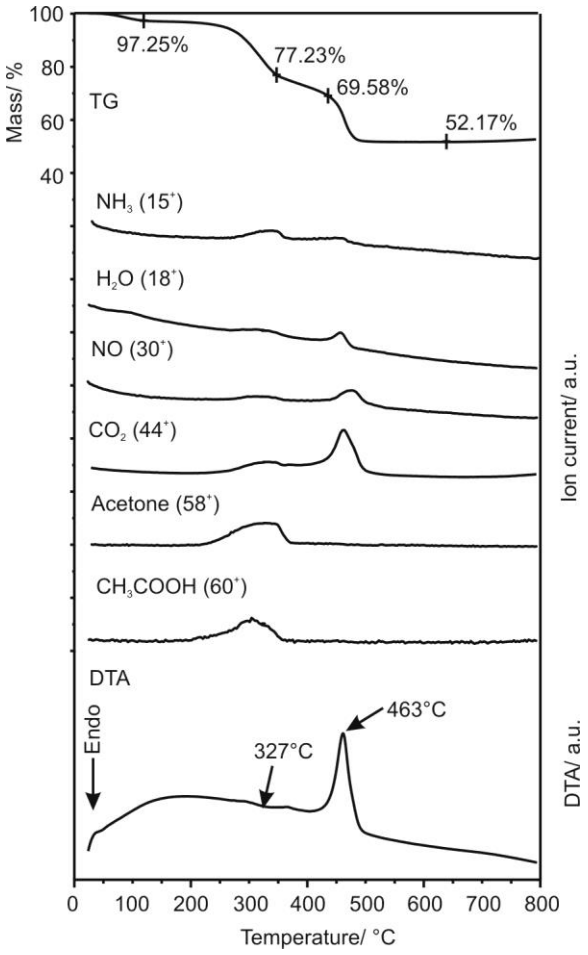
100
80
60
40
Mass/ %
97.25%
77.23%
69.58%
52.17%
TG
NH3 (15+)
H2O (18+)
NO (30+)
CO2 (44+)
Acetone (58+)
CH3COOH (60+)
Ion current/ a.u.
DTA
Endo
327°C
463°C
DTA/ a.u.
0
100
200
300
400
500
600
700
800
Temperature/ °C

Fig. 11

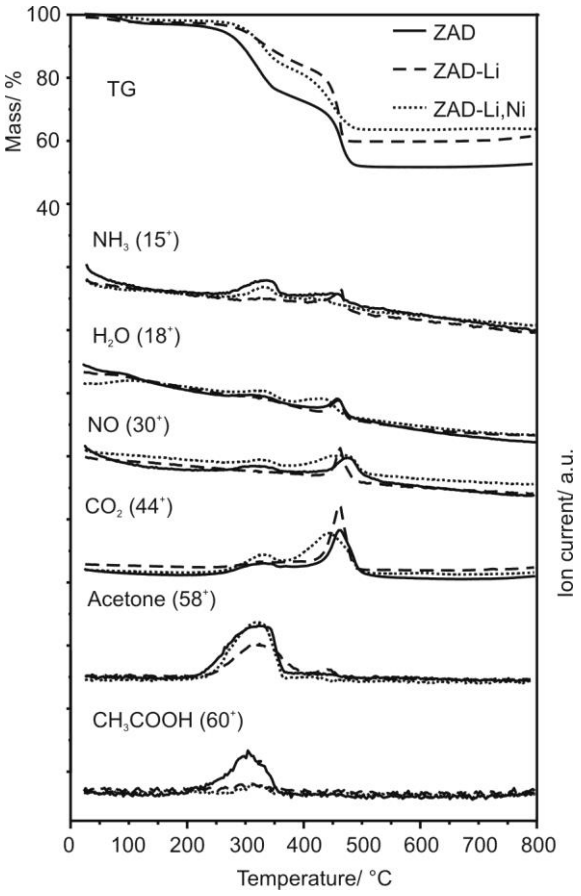
ZAD
ZAD-Li
ZAD-Li,Ni
TG
Mass/ %
100
80
60
40
NH3 (15+)
H2O (18+)
NO (30+)
CO2 (44+)
Acetone (58+)
CH3COOH (60+)
Ion current/ a.u.
0
100
200
300
400
500
600
700
800
Temperature/ °C

Fig. 12

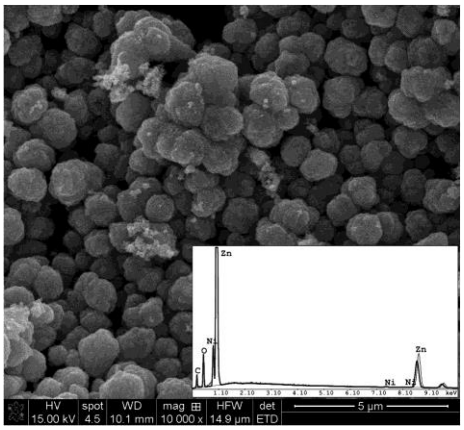
Zn
O
N
C
Ni
Zn
HV
15.00 kV
spot
4.5
WD
10.1 mm
mag
10 000 x
HFW
14.9 µm
det
ETD
5 µm

Fig. 13

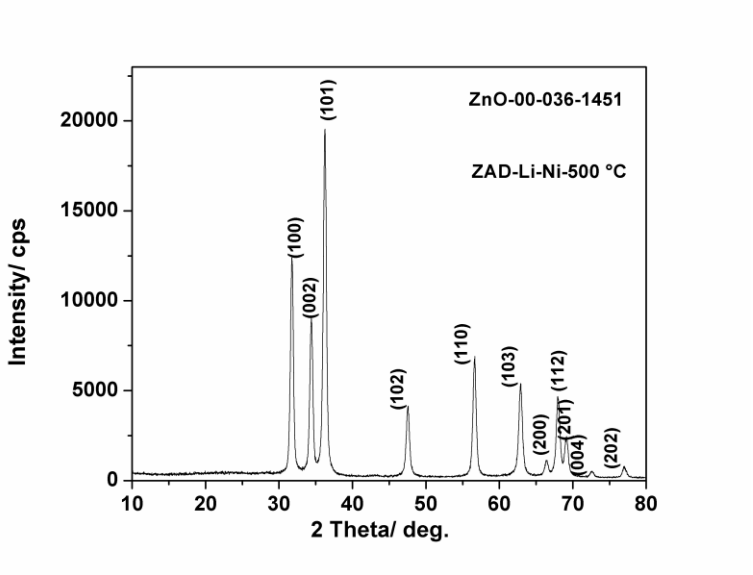
ZnO-00-036-1451
ZAD-Li-Ni-500 °C
Intensity/ cps
2 Theta/ deg.
(100)
(002)
(101)
(102)
(110)
(103)
(200)
(112)
(201)
(004)
(202)

Fig. 14

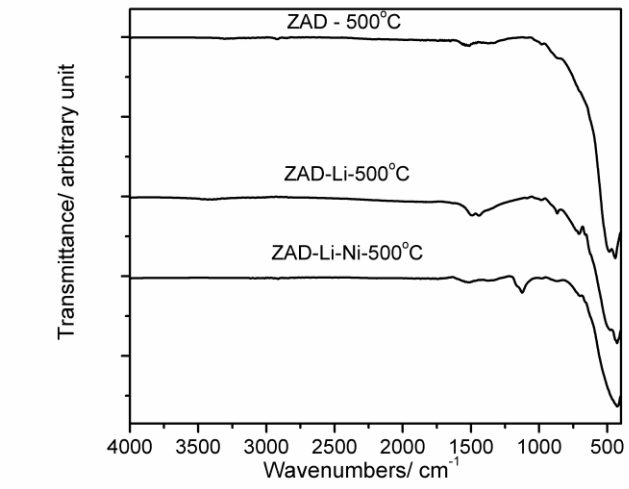
ZAD - 500°C
ZAD-Li-500°C
ZAD-Li-Ni-500°C
Transmittance/ arbitrary unit
Wavenumbers/ cm-1

Fig. 15